

WALK-MAN Humanoid Robot: Field Experiments in a Post-earthquake Scenario

F. Negrello¹, A. Settimi², D. Caporale², G. Lentini², M. Poggiani², D. Kanoulas¹,
L. Muratore^{1,4}, E. Luberto², G. Santaera², L. Ciarleglio³, L. Ermini³,
L. Pallottino², D. Caldwell¹, N.G. Tsagarakis¹, A. Bicchi^{1,2}, M. Garabini² and M.G. Catalano¹

Abstract—Nowadays human intervention is the only effective course of action after a natural or artificial disaster. This is true both for the relief operations where search-and-rescue of survivors is the priority, and for subsequent activities such as the ones devoted to building assessment.

In these contexts the use of robotic systems would be beneficial to drastically reduce operators' risk exposure.

The readiness level of the robots still prevents their effective exploitation in relief operations, that are highly critical and characterized by severe time constraints.

On the contrary current robotic technologies can be profitably applied in procedures like building assessment after an earthquake. To date, these operations are carried out by engineers and architects who inspect numerous buildings over a large territory, with a high cost in terms of time and assets, and with a high risk due to aftershocks.

The main idea is to have the robot acting as an alter-ego of the human operator, who, thanks to a virtual reality device and a body tracking system based on inertial sensors, teleoperates the robot.

The goal of this paper is to exploit the perception and manipulation capabilities of the WALK-MAN robot for building assessment in areas affected by earthquakes. The presented work illustrates the hardware and software characteristics of the developed robotic platform, and results obtained with field testing in the real earthquake scenario of Amatrice, Italy. Finally considerations on the experience and feedback provided by civil engineers and architects engaged in the activities are reported and discussed.

I. INTRODUCTION

Over the past few years, the high number of disasters, such as the Fukushima Daiichi nuclear accident, has raised the attention towards the development and deployment of search and rescue robotic platforms in disaster scenarios [1]. Earthquakes may often lead to structural integrity failures where buildings may be breaking, tearing apart, or collapsing. As an example of such kind of disaster it is possible to consider the data of the recent earthquake in Amatrice, Italy (Fig. 1). On August 24, 2016, a severe 6.0-magnitude earthquake followed by at least 5 aftershocks, ranged between 5.9 and 6.5-magnitude, took place in Italy and affected 4 different

This work is supported by the WALK-MAN FP7-ICT-2013-10 European Commission project.

¹Research Center "Enrico Piaggio", University of Pisa, Largo Lucio Lazzarino 1, 56126 Pisa, Italy

²Department of Advanced Robotics, Istituto Italiano di Tecnologia, via Morego, 30, 16163 Genoa, Italy

³ Protezione Civile Citta Metropolitana Firenze.

⁴School of Electrical and Electronic Engineering, The University of Manchester, M13 9PL, UK

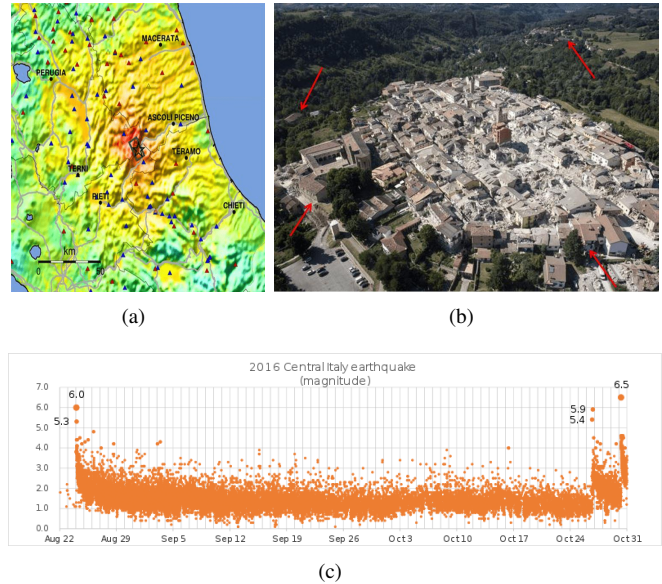


Fig. 1. An overview of the seismic event in Italy in August 2016: a) the area affected by the earthquake with a color scale based on the moment magnitude, b) the town of Amatrice (earthquake epicentre). The central part is completely destroyed, while the buildings of the peripheral areas (red arrows) resisted, and c) the earthquake magnitude data, from August to October [source: Istituto Nazionale di Geofisica e Vulcanologia (INGV)].

regions (Lazio, Abruzzo, Umbria, and Marche) and 180 municipalities. This set of earthquakes was the biggest in Italy over the last three decades and affected more than 25000 people (that had to be evacuated from their houses) and more than 62000 buildings.

Rescuers intervention in this scenario usually is characterized by two separate phases: 1) the rescue and assistance of the people that are trapped under the rubbles or that are injured and 2) the technical assessment of damaged buildings and the assistance to inhabitants who need to recover items from their houses. The rescue phase is always immediate, given that the operation time may affect the life of the people in danger. On the contrary, the second phase usually takes weeks or months, where a limited number of technical experts enter for inspection all the damaged buildings in the affected area (Fig. 1(b)). This procedure has to be also repeated after every aftershock effect (Fig. 1(c)¹). During

¹<http://webservices.rm.ingv.it>

both these phases the emergency responders involved are under high risk, due to the fact that they need to enter partially collapsed buildings or severely damaged masonries. Traversing doors, narrow passages, and areas obstructed by rubbles or objects scattered on the ground make the indoor environment very complex and the operations lengthy and tiresome.

Unfortunately there exist events in the recent past that show how dangerous and critical could be this kind of work. On September 26, 1997, some technicians were inspecting the status of the Basilica di San Francesco in Assisi, Italy, after an earthquake. In that moment, an aftershock caused a collapse of the Basilica, causing the death of four of them.

To support or replace humans in dangerous operations, robotic platforms should possess human-like capabilities, especially concerning locomotion and manipulation skills, for traversing rubble, clearing paths and objects retrieving [2], [3]. Research in this field has been fostered through the organization of several competitions such as RoboCup Rescue, Eurathlon and Darpa Robotics Challenge. In these contests, robots had to face a sequence of tasks inspired by real scenarios, which highlighted different aspects and challenges related to emergency operations.

Search and rescue robotics activities in real scenarios have been mainly focused on providing 3D mapping of the environment or human localization [4], [5]. Often, these systems provide an integrated and intuitive interface for users that are not roboticists. In [1], the key features for search and rescue robots are summarized as survivability, mobility, sensing, communication, and operation.

Moreover, **since** autonomous operations in complex unstructured environments **may** require extensive programming effort to consider all the environmental constraints and **often robots cannot cope with** unforeseen events. An **emerging alternative** approach for these tasks is to provide intuitive interfaces to the pilot for teleoperating the robot [6]. Similar approaches have been presented in various other fields such as space [7] or surgery [8], [9].

Recent developments on legged locomotion for full-body humanoid or animaloid robots, although are very promising, do not show reliable and robust enough performance yet for these environments, especially in tasks with time execution constraints, as demonstrated by the DARPA Robotics Challenge held in 2015.

The FP7 European project WALK-MAN² is focused on developing a humanoid robot that can address several of the aforementioned challenges that may arise in a disaster scenario. In this project we collaborate with the local civil defense corps (Protezione Civile Città Metropolitana di Firenze) to identify the requirements and application technologies for a humanoid robot that needs to take part in an intervention disaster scenario, such as after an earthquake.

This paper presents a use-case for humanoid robots in post-earthquake scenarios, i.e. their use as avatars for remote inspection, damage assessment, and object retrieval. We

discuss the mission specifications coming from civil defense operators, present the system setup and a novel, intuitive and immersive teleoperation interface designed to address this challenge, and finally report on the results of the on-site testing. While a detailed description of the WALK-MAN hardware and software architecture can be found elsewhere [10], this paper focuses on the modifications and development of new components to address the challenges posed by a very specific use-case in post-earthquake scenario.

Given the critical aspects of a rescue task compared to the stability and time constraints of a robotic system, it is still unrealistic to approach the first-phase of intervention. Hence, our work has been devoted to field testing of the perception and manipulation capabilities required to tackle the operations related to the second phase as described above.

For this scope we developed a robotic platform based on the WALK-MAN robot technology, which consists of a wheeled base and a humanoid upper-body. In this way both perception and manipulation tasks can take place during the operation. Its compliant arms, with under-actuated end effectors, provide a sturdy hardware for adaptive and powerful manipulation. At the same time its perception capabilities together with the teleoperation interfaces for vision and bimanual manipulation, provide the pilot with a set of tools for remote building assessment. Thanks to the introduced platform the operators can remotely assess the building damage level through the evaluation table of the standard post-earthquake form [11] and, possibly, the data collected can be streamed to a remote consulting engineering firm where a deeper analysis on the structural integrity of the building can be performed post-processing the data.

The wheeled base has been designed to focus on the assessment activities with a teleoperated robot, reducing the complexity of the system with respect to teleoperated control of legged locomotion.

In the paper we present a description of the hardware platform, the software control architecture, the teleoperation interface that was used to complete several dexterous tasks, and the results of the building inspection. The system effectiveness was demonstrated both in the laboratory and during several field tests³. Finally, we report end-users feedback that was collected from the experts of Protezione Civile Città Metropolitana di Firenze and of the Amatrice Municipality during the field tests.

II. MISSION OBJECTIVES AND REQUIREMENTS

Thanks to the support of the Italian Protezione Civile Città Metropolitana di Firenze, real field testing was organized in Amatrice in one of the buildings affected by the earthquake (Fig. 2(a)).

The focus of the field activity was to evaluate the feasibility of the following tasks:

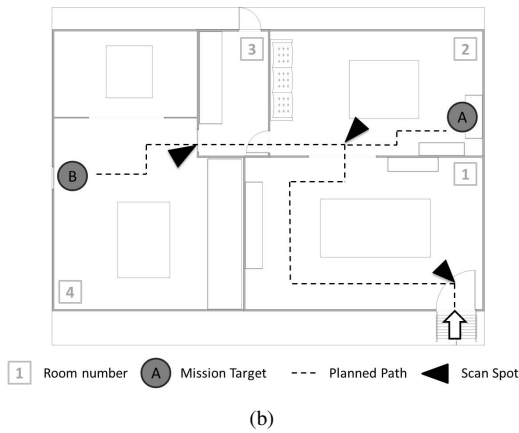
- Build a 3D map of the house interior status.
- Measure the building structural damages.

²<http://www.walk-man.eu/>.

³Video footage of the robot deployment on site at Amatrice <https://www.youtube.com/watch?v=o0Wur7CnesQ>.



(a)



(b)

SECTION 4 Damage to structural elements and existing short term countermeasures

Structural component	DAMAGE (1)											EXISTING SHORT TERM COUNTERMEASURES					
	04-06 Very Heavy			02-03 Medium-Severe			01 Light			Null		None	Removal	Ties	Repair	Propping	Barrier or passage protection
	> 2/3	1/3 - 2/3	< 1/3	> 2/3	1/3 - 2/3	< 1/3	> 2/3	1/3 - 2/3	< 1/3								
1 Vertical structures	<input type="checkbox"/>	<input type="checkbox"/>	<input type="checkbox"/>	<input type="checkbox"/>	<input type="checkbox"/>												
2 Floors	<input type="checkbox"/>	<input type="checkbox"/>	<input type="checkbox"/>	<input type="checkbox"/>	<input type="checkbox"/>												
3 Stairs	<input type="checkbox"/>	<input type="checkbox"/>	<input type="checkbox"/>	<input type="checkbox"/>	<input type="checkbox"/>												
4 Roof	<input type="checkbox"/>	<input type="checkbox"/>	<input type="checkbox"/>	<input type="checkbox"/>	<input type="checkbox"/>												
5 Infill and partitions	<input type="checkbox"/>	<input type="checkbox"/>	<input type="checkbox"/>	<input type="checkbox"/>	<input type="checkbox"/>												
6 Pre-existing damage	<input type="checkbox"/>	<input type="checkbox"/>	<input type="checkbox"/>	<input type="checkbox"/>	<input type="checkbox"/>												

SECTION 5 Damage to non-structural elements and existing short term countermeasures

Damage	PRESENT	EXISTING SHORT TERM COUNTERMEASURES					
		None	Removal	Propping	Repair	No entry	Barrier or passage protection
1 Falling of plaster, coverings, false-ceilings	<input type="checkbox"/>	<input type="checkbox"/>	<input type="checkbox"/>	<input type="checkbox"/>	<input type="checkbox"/>	<input type="checkbox"/>	<input type="checkbox"/>
2 Falling of tiles, chimneys...	<input type="checkbox"/>	<input type="checkbox"/>	<input type="checkbox"/>	<input type="checkbox"/>	<input type="checkbox"/>	<input type="checkbox"/>	<input type="checkbox"/>
3 Falling of eaves, parapets...	<input type="checkbox"/>	<input type="checkbox"/>	<input type="checkbox"/>	<input type="checkbox"/>	<input type="checkbox"/>	<input type="checkbox"/>	<input type="checkbox"/>
4 Falling of other internal or external objects	<input type="checkbox"/>	<input type="checkbox"/>	<input type="checkbox"/>	<input type="checkbox"/>	<input type="checkbox"/>	<input type="checkbox"/>	<input type="checkbox"/>
5 Damage to hydraulic or sewage systems	<input type="checkbox"/>	<input type="checkbox"/>	<input type="checkbox"/>	<input type="checkbox"/>	<input type="checkbox"/>	<input type="checkbox"/>	<input type="checkbox"/>
6 Damage to electric or gas systems	<input type="checkbox"/>	<input type="checkbox"/>	<input type="checkbox"/>	<input type="checkbox"/>	<input type="checkbox"/>	<input type="checkbox"/>	<input type="checkbox"/>

(c)

Fig. 2. Overview of the mission organization: a) the inspected house and the location of the outdoors pilot station, b) the inspected building layout and the mission plan (the mission objectives, the planned path, and the spot suitable for room scansion are indicated), and c) a part of the building assessment standard form.

- Recover some objects from the house.
- Install monitoring systems and sensors inside damaged building.

As for the last point, the technical experts involved sug-

gested the use of the robot to place indoor wall position sensors that monitors building movement and to equip the robot with additional sensors, such as multi gas detector or thermal camera.

Fig. 2(b) shows an overview of the inspected four-rooms house, which includes several connecting doors. Two indoor mission targets were a priori defined: an object to be retrieved in spot (A) and a door to be opened in spot (B). To complete the tasks, we plotted a mission plan (Fig. 2(b)) in order to find a path for 1) reaching the mission targets and 2) reaching suitable locations to perform a room scan. A possible path is shown by the dotted line, whose action feasibility was every time verified on-line by the robot operators.

During the robotic field tests, a group of technical experts was close to the pilot station to perform the building evaluation remotely through the robotic platform. The building assessment is normally done by filling a suitable technical form following the post-earthquake procedures [11]. Fig. 2(c) shows excerpts of the forms that the technical team has to fill for each inspected building. It is worth noticing that such forms are meant for a fast and qualitative evaluation of the building structural conditions (i.e. Fig. 2(c) Section 4: very heavy, medium and light damage). The information to report is essential and strongly oriented towards short term countermeasures (right part of the table in Fig. 2(c)), which are evaluated based on the experience of the operator and supported by the measurements that can be taken on the field (i.e. measurement tape). The analysis of these forms provides very useful guidelines to develop specifications for the robotic mission. Accordingly, our aim was to provide the operator with an appropriate sensory feedback as he was personally inspecting the building, together with the possibility to extract basic quantitative measurements (point-to-point distance or angles among planes). Moreover, the assessment forms concern both the damage to structural (walls, roof etc.) and non-structural elements such as hydraulic or gas pipelines and electrical systems. Especially to detect the latter (Fig. 2(c) Section 5), given the limitation of autonomous recognition systems, it is essential to have the human in the loop, to perform an evaluation based on his expertise.

In order to define the mission requirements, our design team went in the town of Amatrice one month before the official mission, to visit the areas affected by the earthquake. Fig. 3 reports some of the pictures taken during the inspection. Among the normal households features (i.e. doors, tables etc.), the main characteristics of a post-earthquake scenario are the debris on the ground, the collapsed furniture that limits the accessibility to the rooms and the damages to the building structure.

The joined information provided by the form and the inspection to the house interior status, were used to define the hardware specifications of the robotic platform, which are synthetically reported in Tab. I. The requirements are divided in five domains, which define the specifications of the different subsystems that constitute our robotic platform: perception, manipulation, mobility, autonomy and



Fig. 3. The house interior status. In the pictures it is possible to recognize doors, objects scattered on the ground, collapsed furniture and items obstructing the vision.

user interface for teleoperation. Specifications contained in Tab. I, represent the input for the following sections where the implementation of the setup is discussed.

III. ROBOTIC PLATFORM SETUP

The mission field has been organized in three areas (Fig. 4(c)): the remote Pilot Station (a), the outside zone peripheral to the building (b) and the indoor zone (c), where the robot operated. The overall infrastructure has been organized as reported in Fig. 4(a). The components that belong to the robot and operators side are reported on the left and right part of the figure, respectively. Two ethernet cables, one dedicated to the control data and one dedicated to the vision data, has been connected to two wireless routers, one near the pilot station and one near the entrance of the building. In this way the robot remotely received commands and sent back to the teleoperator the visual streaming.

A. Robot

For this mission, we developed a prototype robotic platform based on the WALK-MAN **robot design technology [10] and on the specifications determined by the scenario requirements, listed on Tab. I. The robot** consists of a wheeled base for better stability and a humanoid upper-body for visual inspection and manipulation task completion (Fig. 4(b)). The overall size of the platform is crucial for this application due to the restricted indoor passages, moreover it defines the mobility capabilities of the robot. In particular, the width of its base determines the minimum allowed corridor size, while its length affects the turning radius of the mobile base. For these reasons the robot was provided with the smallest mobile base available on the market and comparable with the upper-body weight and size. Overall dimensions are reported in Fig. 4(b).

The end-effectors are based on the Pisa/IIT SoftHand [12], so that they increase the robustness, reliability, and efficiency of the manipulation system, while reducing its mechanical and control complexity. Each end-effector is equipped with a 6 axis force/torque sensors that provide feedbacks for the manipulation tasks.

The exteroceptive visual perception system of the robot is a MultiSense-SL⁴ integrated in the robotic head. It includes a stereo RGB camera, a rotating 2D lidar scanner and an IMU sensor. We set the resolution of the stereo camera to 1Mpx for the RGB-D data with an update rate of 15Hz, while the laser scanner returns 1024 points at 60Hz and rotates at 1rad/s. A ZED stereo camera⁵ is placed on top of the robotic head and returns images of the reconstructed 3D environment to the pilot station for teleoperation and inspection purposes. To cope with the variety of light condition in post-earthquake scenarios, the robot head is equipped with 4 LED units (brightness 690lm/unit, power 6W/unit). Their strobing and light intensity can be actively controlled by the pilot to tune them according to the needs.

The robot is powered by a custom Li-On battery (29V-63Ah) that provides it about 3 hours of power autonomy.

B. Pilot Station and Teleoperation Interfaces

The WALK-MAN pilot interface [13] has been used by the operator to send high level commands to the robot and visualize its kinematic state, which is displayed in the 3D environment surrounding it (Fig. 5). Moreover a monocular scene image was visualized in the interface.

A custom Human Machine Interface (HMI) has been realized to teleoperate the robot (Fig. 4(a)). The HMI was composed of an immersive 3D viewer and four inertial and electro-myographic bracelet sensors to control the movement of the robot arms and hands. The Myo bracelets⁶ have been used to acquire the teleoperator's EMG and inertia measurements. We decided to place one Myo bracelet on the forearm and one on the bicep of the pilot. A Madgwick filtering algorithm [14] has been used to obtain the orientation of each Myo. Hence, the relative orientation between the two devices is used to calculate the wrist pose given the length of the pilot's arms. Finally, a linear combination of electromyographic signals from the forearms are processed, as reported in [15], to extract a signal used as a reference for the control of the robot's hand closure. This method also allowed us to cope with the issues of placement and repeatability of EMG sensors, since each operator follows a short training session (one or two minutes) to obtain a mapping from the EMG signals to hand closure signals. More information about the use of EMG sensors for controlling the Pisa/iit SoftHand can be found in [16]. Virtual reality viewer Oculus Rift⁷ has been used to exploit the humans stereo vision and reproduce 3D scenes, its inertial unit and Infra-Red (IR) sensors have been used to estimate its pose in the

⁴<http://carnegierobotics.com/multisense-sl/>

⁵<https://www.stereolabs.com/zed/specs>

⁶<https://www.myo.com>

⁷<https://www3.oculus.com/en-us/rift>

TABLE I
HARDWARE REQUIREMENTS AND SPECIFICATIONS FOR REMOTE OPERATIONS IN DISASTER SCENARIOS.

Tasks & Requirements	Domain	System Specifications	Implementation
<ul style="list-style-type: none"> • Mapping and Measuring, to extract visual data in different conditions. • Possibility to operate during night or with no light sources. • Possibility to scan a room without moving or reorienting the robot base. 	Perception	<ul style="list-style-type: none"> * Redundant vision sensors. * Lighting systems. * Pan and tilt rotation of cameras and sensors. 	<ul style="list-style-type: none"> ψ MultiSense-SL (rotating 2D LiDAR, stereo camera and RGB video). ψ ZED stereo camera. ψ 4x visible light LEDs, integrated in the MultiSense-SL. ψ 2 DOF neck (pitch and yaw) and 1 DOF waist (yaw).
<ul style="list-style-type: none"> • Capability of grasping objects with different characteristics (shape, weight, stiffness, etc.). • Obstacle and path clearance. • Safe contacts and interactions. • Capability to survive strong interaction with the environment. 	Manipulation	<ul style="list-style-type: none"> * Grasping tool for a wide range of objects. * Manipulator arm. * Knowledge of the forces exchanged with the environment. * Tactile sensing. * Physical sturdiness. 	<ul style="list-style-type: none"> ψ Underactuated compliant hand. ψ Dual arm system (7 DOF each). ψ Force/Torque sensors at the end effectors. ψ Under development. ψ Compliance at the joint level.
<ul style="list-style-type: none"> • Navigation in confined spaces, such as houses, offices and shops. • The building structure can be compromised by vibrations. • Indoor operations. • High stability over small sized debris. 	Mobility	<ul style="list-style-type: none"> * Limited footprint. * Limited vibration emissions. * Limited pollutant emissions. * Intrinsically stable mobile base. 	<ul style="list-style-type: none"> ψ Footprint 810mm x 1040mm. ψ Electrical Actuation. ψ Four wheel mobile base.
<ul style="list-style-type: none"> • Remote deployment inside damaged building. • Operative range within 100m from the pilot station. • Power autonomy >1 hour. 	Autonomy	<ul style="list-style-type: none"> * Untethered communication. * Onboard battery. 	<ul style="list-style-type: none"> ψ Indoor: wireless communication (WLAN). ψ Outdoor: wired connection to field routers (Ethernet). ψ Custom Li-On battery.
<ul style="list-style-type: none"> • First person user experience. • Operator comfort for extended missions. 	User Interface	<ul style="list-style-type: none"> * Immersive 3D stereoscopic visual feedback. * Low latency. * Pilot motion capture. * Wearable and portable device. * Lightweight and highly integrated. * Tactile rendering. 	<ul style="list-style-type: none"> ψ Oculus Rift. ψ 4x Myo bracelets. ψ Under development.

space. The stereo images coming from the Zed camera were sent to the 3D viewer for a visual feedback from the robot. The orientation of the teleoperator’s head, used for robot gaze teleoperation, was computed using the inertial sensor placed in the Oculus system. The teleoperator’s wrists’ pose and hands level of closure were sent to the control module that translates the information into control inputs for the robot joints (see Sec. IV-A).

On the communication side, the main computer (PC1) was directly connected to the ethernet cable dedicated to the commands sent by the teleoperator, while the second cable was connected to a router that also establishes a local network between all the pilot PCs, through an ethernet connection. In this way the teleoperator was receiving the visual data in the Oculus Rift while sending his head orientation, wrist pose and hands closure references to PC1. Finally, the Myo bracelets were connected via Bluetooth to their dedicated PCs, where the processing described above was executed to retrieve operator arms’ pose and orientation. Although in the present work it is not specifically addressed, the communication channel plays a paramount role for the achievement of our objectives: in fact, it was shown that high com-

munication delays in visuo-haptic applications (>150ms) significantly degrade performance [17]. For these reasons, as future development we will build a robust and effective communication channel, e.g., refining existing perceptually-motivated compression approaches of the transmitted data (dead band and prediction approaches) to enable a proper information exchange.

C. Software Architecture

Given the target of the mission and the new robot setup, a flexible and easily reconfigurable software platform was needed. We chose the *XBotCore* (Cross-Bot-Core) [18] robot control framework, which satisfies hard Real-Time (RT) requirements, ensuring 1KHz control loop in EtherCAT-based robots. The robot software architecture played a key role in the mission success: it guaranteed control module code reusability and interoperability with the YARP [19] non-RT framework. *XBotCore* is a novel approach to configure low-level control systems by using modern description formats such the URDF⁸ (Universal Robotics Description

⁸<http://wiki.ros.org/urdf>

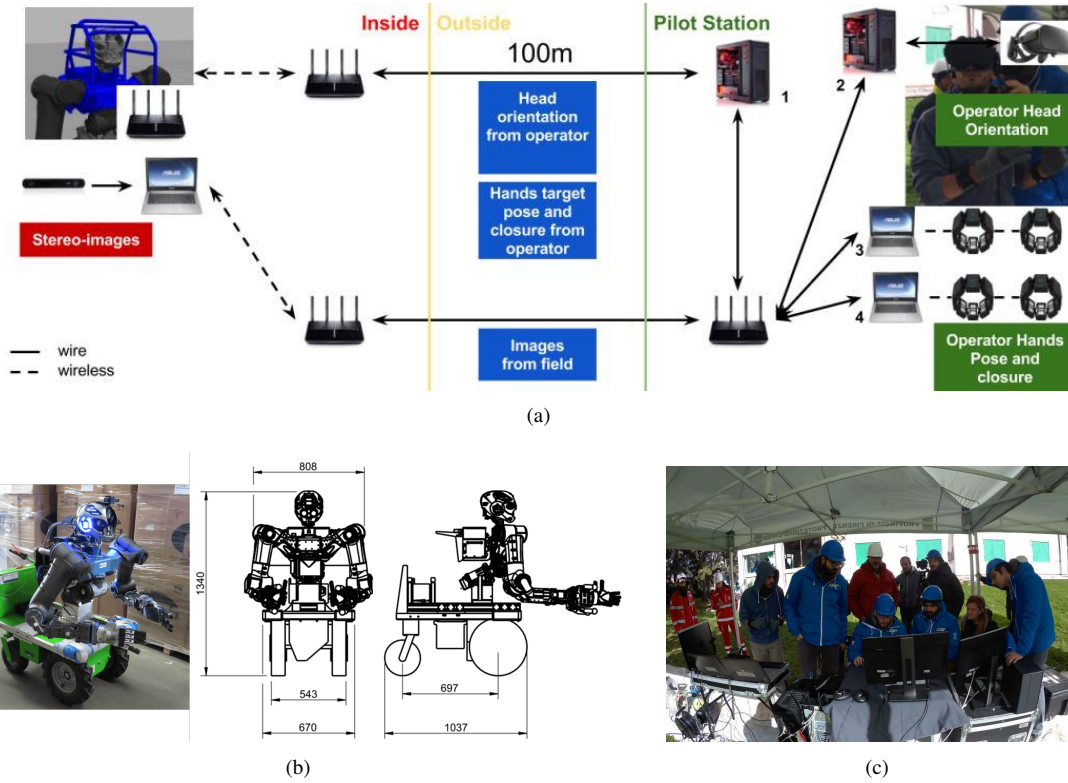


Fig. 4. a) the communication and control architecture scheme, b) The robotic platform, based on the upper-body of the WALK-MAN robot and c) the remote pilot station.

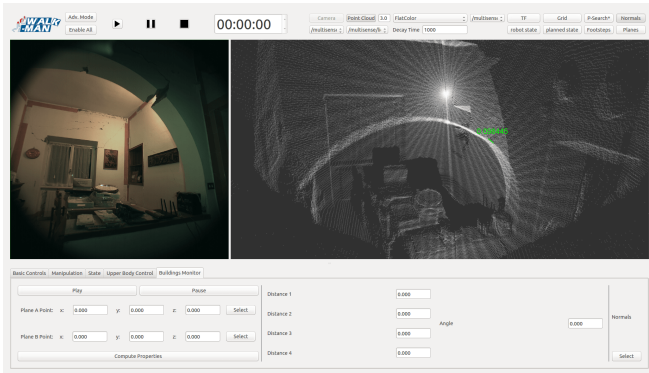


Fig. 5. The Pilot Interface (PI) used by the operator of PC1: the 3D viewer is used to understand the scene and take measurements.

Format) and the SRDF⁹ (Semantic Robotic Description Format) which are traditionally used for high-level software components. Thanks to the introduced abstractions, it is possible to control different robots or different parts of the same robot without code changes: the API provided to control the robot is dynamically built starting from the robot URDF/SRDF. Modifying the SRDF, for instance removing a kinematic chain (e.g. the torso), results in a different API for the user that is compatible with the available/desired parts of the robot to control. We exploited this feature by

⁹<http://wiki.ros.org/srdf>

removing the leg chains from the SRDF and we controlled the humanoid upper-body using a YARP module without any code modification.

IV. CONTROL AND PERCEPTION

A. Teleoperation Module

To remotely control the upper-body of the WALK-MAN robot we developed a dedicated control module, which receives the information needed from the Pilot Station to reproduce the teleoperator movements on the robot. In particular, three kind of data are sent to the control module and then translated to a robot joint motion: the head orientation, the pose of the wrists, and the amount of hands closure.

The quaternion representing the operator's head orientation with respect to the plane perpendicular to the gravity vector is translated, by means of a linear map, in the yaw and pitch joint of the head and in the yaw joint of the torso. The rotation corresponding to the roll angle has not been considered. For each arm of the teleoperator, using the two MYO Armband bracelets relative orientation, the cartesian pose of the wrist with respect to the shoulder is computed. This pose is then scaled to map the human arm to the robot arm and it is sent through the network. When the pose is received by the control module, a Jacobian-based inverse kinematics is performed, obtaining the desired arm joints position. Note that at the system start-up the teleoperator assumes a predefined homing position to define the relative position of the two MYOs.

Thanks to the EMG sensors of the MYO Armband bracelets, a value proportional to the signal representing the muscular activity on each forearm is obtained using a linear map. This value represents the desired positions for the hand motor. This is very convenient for the human operator: since the MYO bracelets are positioned on the forearm, a muscular activity can be generated by opening and closing the hand; consequently the robot will move the hand as the teleoperator does. The obtained desired joints position for the hands, arms, torso, and head joints are then sent to the low level controller of the motor boards, resulting in a robot motion. In each part of this control scheme, safety bounds are checked before moving the robot, in order to avoid self-collisions. A tuning phase for each teleoperator takes place before the experiments, since each person is characterized by different electro-myographic signals. During this phase the teleoperator is required to raise the arms and keep them fixed in a straight pose for 3s.

B. Vision Module

To visually examine the inspected building we used the exteroceptive sensors, i.e. LiDAR and RGB-D cameras, to acquire crucial information about the structure of the indoor environment. For this purpose we developed two different vision processing modules dedicated to different measurements acquisition.

1) *Plane Detection Module*: The first module has been developed to analyse the structure of the scene by searching for planar regions in it. If the extracted planes are bigger than a certain threshold, they are categorized in four different types: ceiling, floor, frontal and lateral wall. This categorization is necessary for inspection in disaster scenario, for instance to recognize cracks or anomalous inclination of walls, see Fig.6. For the classification, the relative orientation between the planes and the robot head is used. Moreover, the pilot can compare the relative distance and orientation of two planes by selecting them through the Pilot Interface.

The plane estimation algorithm uses as input the LiDAR data provided by the rotating laser scanner of the MultiSenseSL head. The point cloud that has been used for plane classification is obtained by acquiring and accumulating 10s of laser data in order to allow a whole environment scanning (Fig. 8(a)). Then, the point cloud is filtered using a 3D pass-through filter to remove image regions that are out of our interest. A statistical outlier and a downsampling filter is also applied on the point cloud dataset, using a voxelized grid approach. In this way, the laser image has a reduced number of points allowing a faster plane detection. The estimation uses the RANSAC algorithm [20] to search for the best plane in the cloud, reducing at the same time the number of iterations, even if the number of points is very large. Points belonging to the same plane are removed from the original laser point cloud in every iteration, until a specified number of points threshold is met. Then, for each plane the mean normal vector and its four corners are computed in order to classify a plane as ceiling, floor, lateral or back wall, visualized in different colors in Fig. 8(b). Upon request,

the pilot can use a ROS service to compute the relative orientation of planes and the distances between identified planes corners, computed along the normal direction.

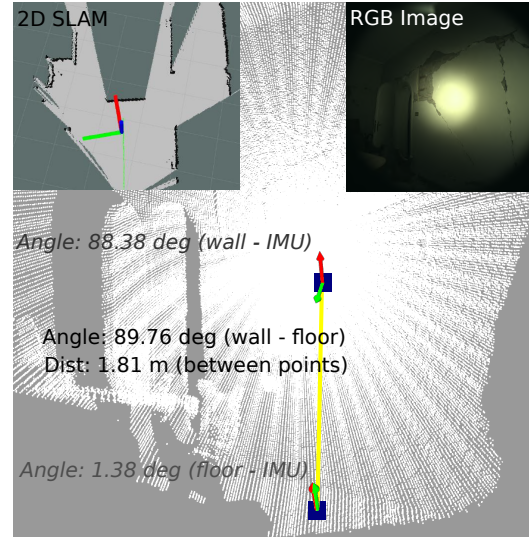


Fig. 6. Distances and angles between the wall, the floor, and the gravity vector in room 2. On the upper left a 2D LiDAR-based SLAM path and on the right the RGB image on the scene.

2) *Local Regions Measurements Module*: The second vision module is dedicated to compute distances and orientations between selected local regions in the environment, using both the 3D perceptual data from the stereo camera and the LiDAR scanner as well as the gravitational force vector from the IMU sensor that is part of the MultiSenseSL head. For the point cloud data the pilot can select either to accumulate the laser scanner data such that the whole environment is scanned, or to use the filtered stereo RGB-D data. The gravity vector is computed from the IMU data after passing a Madgwick pose filtering in real-time [21]. We analysed the mean and standard deviation IMU rotational error for the estimated gravitational vector, which is 1.8° and 1.1° respectively.

There are two options through the Pilot Interface. First, the pilot can select two seed points in the environment. For each seed point a local r -sphere neighborhood is searched in the point cloud using a KD-Tree structure, where r is preselected by the pilot (in the experiments a sphere of 15cm radius was used). For each neighborhood a circular plane is fitted using the RANSAC algorithm. The relative distances between the two seed points, and the perpendicular distances between the fitted planes are computed, as well as their relative angle, i.e. the angle of their normal vectors. Secondly, the pilot can compare the angle of the local fitted plane with the gravity vector that is extracted from the IMU sensor. In the same time a 2D map of the walls can be created using the SLAM system introduced in [22], by having the LiDAR scan rays parallel to the ground floor. An example of these measurements can be seen in Fig. 6.

Both modules are implemented in C++ as ROS nodes, using the PCL [23], while the second module works in

real-time and is part of the SPL [24]. The thresholds and parameters setting for the filtering and the plane estimations can be tweaked dynamically through a GUI, in order to meet specific demands according to different environments. For instance the point cloud region can be limited to closer-to-robot points, when only planes around the robot are required and not ceilings or floors.

V. RESULTS AND END-USERS FEEDBACK

Fig. 7 summarizes the indoor operations executed by the robot under the supervision of the technical experts. In detail it highlights the locations of the various activities performed during our field tests, like measurements and manipulation tasks.

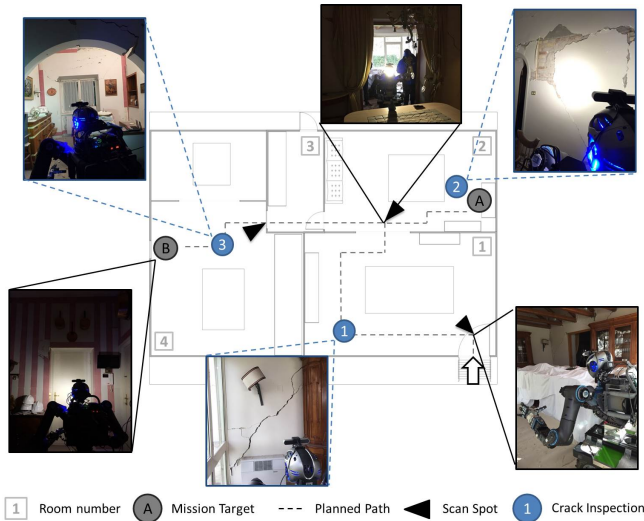


Fig. 7. From room 1 to 4 the robot is shown scanning a room, measuring cracks, manipulating objects and opening a door during the field operations.

A. Measurements Acquisition

Fig. 8(a)-8(b) show the 3D scene sent to the pilot PC1 and the reconstructed planes computed by the dedicated vision module, for the first explored room.

Thanks to the acquired measurements it was possible to evaluate the state of the building. In particular, the representative engineering and architect professionals requested the assessment of the wall inclination with respect to the ground. For all the three rooms the wall inclination with respect to the floor was about 90° ($\frac{\pi}{2}$ radians) and thus the building preserved the structural entirety despite the copious earthquakes. Nevertheless, many cracks were present in the building and to evaluate the damage level we were requested to estimate their width and length. As shown in Fig. 8(c)–8(e) a set of cracks were visible through the Pilot Interface. For those cracks the width estimation measurements were reported and compared with the real crack size which was measured manually on-site. The lidar sensor (Hokuyo UTM-30LX-EW) of the MultiSense-SL system was used for this purpose, given its high accuracy compared to the other range

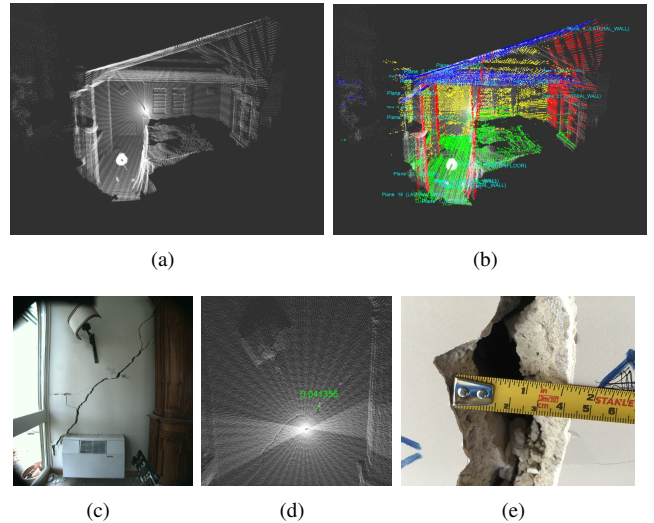


Fig. 8. (a) The 3D point cloud of the first room, (b) the reconstructed planes of the first room, (c) RGB view of a crack inspected in the first room from the Pilot Interface point of view, (d) the crack estimated width measurement in the point cloud (in meters), and (e) the manually measurement of the crack width on the field (in cm).

sensors on the robot. In particular, we tested the accuracy of the lidar point cloud by accumulating the point measurements on a plane and calculating the average distance between two point-neighbors (*lateral accuracy*) as well as the displacement depth of the same point over some fixed time slot (*depth accuracy*). For surfaces 1m from the sensor the lateral accuracy is 6mm, while the depth accuracy is 11mm. While the distance between the sensor and the surfaces increases the accuracy is dropped (± 30 mm for 0.1m-10m as reported in the laser sensor specifications). As it can be seen from the images, the measurements are precise enough, within 6mm, to allow the engineers and the architects to assess the cracks severity, and hence complete the estimation of the building state.

B. Manipulation Tasks

The robot manipulation capabilities were fundamental during indoor operations to get access to the four inspected rooms. The robot opened two doors in the building: one door has been opened by pushing it, and the other one by turning the handle and pulling it (Fig. 9). Another manipulation task consisted in collecting relevant objects (Fig. 10) to be examined successively. All the manipulation tasks took place in teleoperation mode, using only visual feedback to complete the corresponding task. The enhancement of the teleoperation module by adding haptic feedback is currently under study. In Fig. 9 and 10, we report the 6-axis experimental force-torque data acquired during the manipulation tasks. A sequence of images during a remote manipulation task, from the operator and the robot point of view, is reported in Fig. 11.

C. End-users Feedback and Lesson Learned

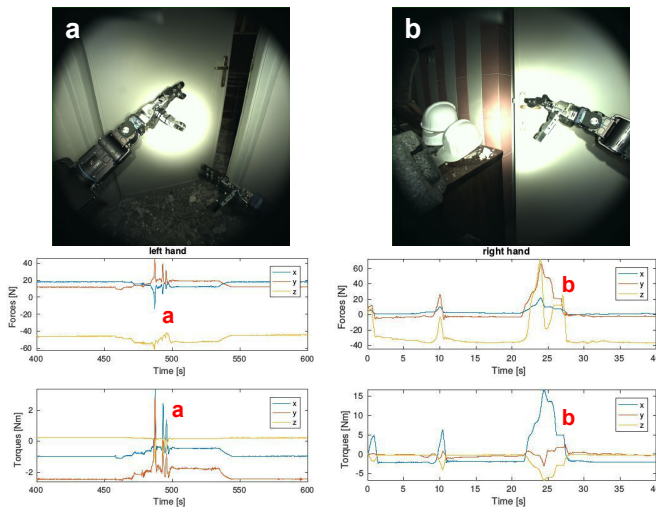


Fig. 9. The WALK-MAN point of view when opening two doors. One door is opened by pushing, and the other by turning the handle and pulling it. For the two cases, the force-torque measurements are reported, where interactions with the environment are clearly distinguishable from the graphs.

During field tests the WALK-MAN team cooperated with the technical groups that usually supervise all the activities. On-site several operators from the Civil Defense (3 operators), the Red Cross (2 operators) and the Amatrice Municipality (2 architects and 1 structural engineer) were present to validate the feasibility of the tasks discussed in Sec.II.

Tasks 1 and 2 concern the visual feedback provided by the interface and the vision modules as tools to retrieve information on the house interior status and quantify the entity of the structural damages. Technical experts assessed on the field the effectiveness of the systems for a first evaluation of the building status, as required by the standard forms reported in Fig. 2(c). Moreover, they confirmed that the use of these tools can go beyond the simple operation of measuring cracks, for example streaming the data collected to a remote consulting engineering firm.

Concerning manipulation tasks, object retrieval (task 3) was demonstrated to be possible, although non trivial, while the sensor placement (task 4) is difficult due to the lack of tactile feedback. Adding it would also enable the teleoperator to perform the sclerometer test which is one of the most common non-destructive test on concrete structures.

The long-term objective is to develop a humanoid system with human like capabilities, since wheeled systems present strong mobility limitation especially when the environment presents large debris/holes or ladders to overcome. In the present application, we decided to implement a wheeled base since legged locomotion was not at the development stage to guarantee safe and robust navigation on uneven terrain. It is worth noticing that, during post-earthquake operations, the main aim is to identify those building that survived the earthquake and can be repaired. The buildings which are partially collapsed or anyway visibly damaged are excluded

from the inspection in order to speed up the operations. Therefore, a large part of the building to inspect do not present large quantities of debris on the ground and wheeled systems can be effectively used, at least to explore the ground floor. As future work we will study the capabilities required to navigate different terrains in order to define guidelines for using either a wheeled or legged systems.

From a hardware point of view, robustness and reliability are required to achieve safe interactions with the environment, while good perception capabilities are essential to support pilot operations.

~~We believe that this approach can~~ **We proposed to control the robot through a teleoperation framework. Aiming with this approach to fill the gap between the robot and the human, unifying the physical performances of the first and the intelligence of the latter. Indeed, scene understanding is a difficult task, and autonomous methods are still far beyond the human capabilities. Another example refers to** **Navigation is particularly challenging** in scenarios with a high level of unpredictability, due to the presence of debris and grounds with different characteristics (stiffness, friction etc.). Teleoperation offers the advantage to rely on pilot experience and perception, for selecting a safe path inside the building or for locating stable footholds, which are very challenging tasks for artificial intelligence. The **robot-control teleoperation interface** was based on the Oculus Rift and Myo bracelets teleoperation framework ~~which are commercial and therefore highly dependable components~~. This resulted in a relatively cheap teleoperation system, where the cost is approximately 5400€ (MYO x4 200€/unit, Oculus x1 600€, Laptop x2 2000€/unit). The presented teleoperation framework will be enhanced in the future using force feedback and other methods to better make the user understand the spatial perception of its avatar, i.e. how far the surrounding objects are.

Concerning the developed communication system, the final aim of such system is to have a completely wireless communication between the pilots and the robot, in order to enhance autonomy. However, to have a good coverage of the area that the robot has to explore, a dedicated infrastructure is needed: this can be achieved by means of wireless routers placed in the environment. Routers can be positioned by humans in safe locations, or by other robots directly inside the dangerous area. These robots should be lighter and simpler than a humanoid (e.g. rovers and drones) and should be equipped with one or more wi-fi antennas. In the future, as already discussed, we will consider to adopt also different communication technologies such as cellular data communication protocols.

~~During the field test we had 3 subjects testing the teleoperation interface: two users with previous experience as robot pilots and a non-expert user. The usage of the proposed platform resulted intuitive and after receiving little instructions from the main robot operator, they were able to inquire for specific measurements or tests that could help them better understand the status of the building. Based on~~

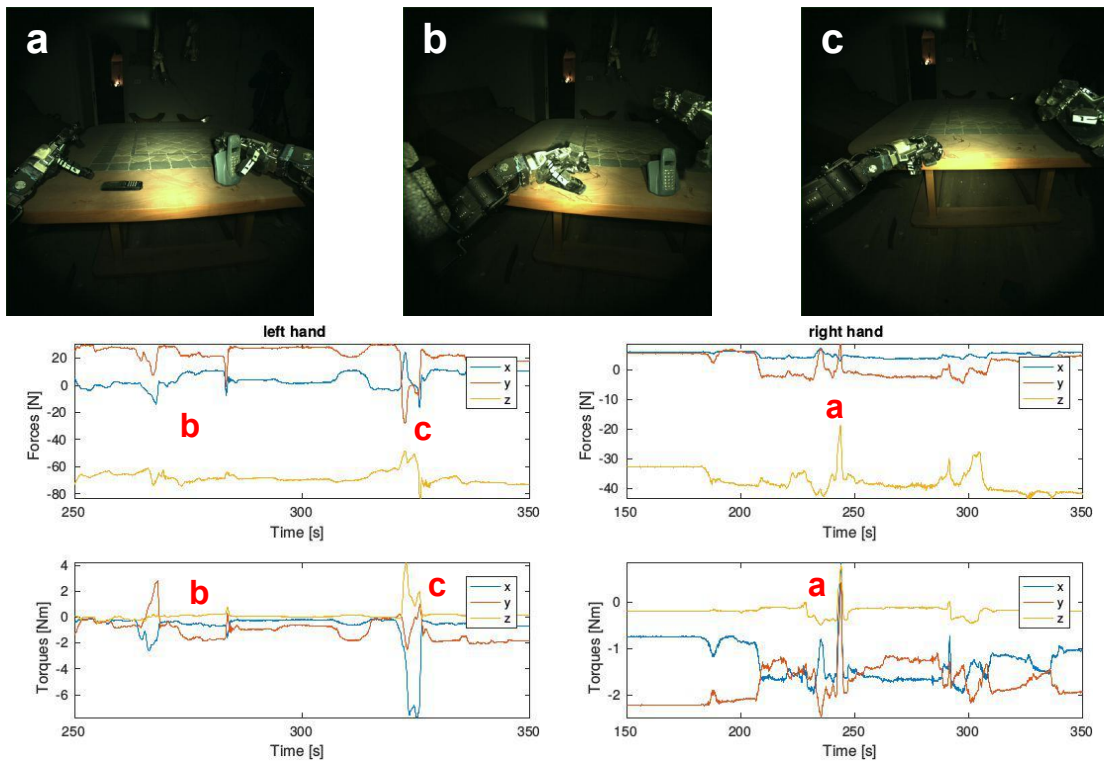


Fig. 10. The WALK-MAN point of view when collecting different objects, using different strategies. The force-torque measurements are reported to highlight the interactions of the robot with the environment.



Fig. 11. A detail of a manipulation task executed during the field test. On the top line the pilot station is visible, with the operator wearing the Oculus and Myo bracelets, while in the bottom line the robot WALK-MAN executes the commanded actions.

~~the subjects feedback, we improved the teleoperation interface and the general control architecture. This preliminary investigation of the functionality of the~~

~~proposed device is to be considered as a first step toward a deeper usability analysis which will be considered in our future developments.~~

Future work will consider, **on one side, a usability analysis to assess the easiness of use of the teleoperation framework, on the other side**, the use of sensing redundancy and the implementation of fail recovery mechanisms to further increase the robustness and **the dependability of the whole system in real conditions.**

VI. CONCLUSIONS

In this work we reported the results of the field test in a building damaged by an earthquake for evaluating the technologies developed inside the WALK-MAN project, with a special focus on perception and manipulation readiness. We successfully visually inspected four rooms performing several manipulation activities, both for object retrieval and for path clearing (e.g. door openings). From our perspective, on site testing is the best way to validate the maturity of newly developed technologies and to identify critical aspects to improve towards real advancement in the field of search and rescue robotics. Finally the evaluation of the technical experts present on site was very positive and confirmed that this technology can address a real issue. Moreover, through a centralized control station far from the dangerous environment, visual information is collected to be evaluated by experts. Having multiple parallel working robotic platforms in various buildings with a centralized monitoring station may speed up the whole second phase operations. Ongoing research is related to extend the current work enabling teleimpedance control on the robot. Using the electromyographic sensors the operator can change the stiffness of the related robotic arm using his muscular activity. This will allow to execute remotely, using the same teleoperation framework, different tasks that require a different level of robot stiffness. Moreover, the design of a control framework for teleoperated legged locomotion is under study and will be a key element to enhance the effectiveness of the WALK-MAN platform in the disaster scenarios.

ACKNOWLEDGMENTS

The development of WALK-MAN platform is supported by the WALK-MAN FP7-ICT-2013-10 European Commission project. The authors want to acknowledge Protezione Civile Città Metropolitana di Firenze for the support during all the activities described in this work. Finally an acknowledgment to Andrea di Basco and Marco Migliorini for their support in the development of the hardware prototype.

REFERENCES

- [1] Liu Jinguo, Wang Yuechao, Li Bin, and Ma Shugen. Current research, key performances and future development of search and rescue robots. *Frontiers of Mechanical Engineering in China*, 2(4):406–416, 2007.
- [2] J. S. Mehling, P. Strawser, L. Bridgwater, W. K. Verdeyen, and R. Rovekamp. Centaur: Nasa’s mobile humanoid designed for field work. In *Proceedings 2007 IEEE International Conference on Robotics and Automation*, pages 2928–2933, April 2007.
- [3] Max Schwarz, Tobias Rodehutsors, David Droschel, Marius Beul, Michael Schreiber, Nikita Araslanov, Ivan Ivanov, Christian Lenz, Jan Razlaw, Sebastian Schüller, et al. Nimbros rescue: Solving disaster-response tasks with the mobile manipulation robot momaro. *Journal of Field Robotics*, 2016.

- [4] Nathan Michael, Shaojie Shen, Kartik Mohta, Yash Mulgaonkar, Vijay Kumar, Keiji Nagatani, Yoshito Okada, Seiga Kiribayashi, Kazuki Otake, Kazuya Yoshida, et al. Collaborative mapping of an earthquake-damaged building via ground and aerial robots. *Journal of Field Robotics*, 29(5):832–841, 2012.
- [5] Geert-Jan M Kruijff, Fiora Pirri, Mario Gianni, Panagiotis Papadakis, Matia Pizzoli, Arnab Sinha, Viatcheslav Tretyakov, Thorsten Linder, Emanuele Pianese, Salvatore Corrao, et al. Rescue robots at earthquake-hit mirandola, italy: A field report. In *Safety, Security, and Rescue Robotics (SSRR), 2012 IEEE International Symposium on*, pages 1–8. IEEE, 2012.
- [6] Kapil D Katyal, Christopher Y Brown, Steven A Hechtman, Matthew P Para, Timothy G McGee, Kevin C Wolfe, Ryan J Murphy, Michael DM Kutzer, Edward W Tunstel, Michael P McLoughlin, et al. Approaches to robotic teleoperation in a disaster scenario: From supervised autonomy to direct control. In *2014 IEEE/RSJ International Conference on Intelligent Robots and Systems*, pages 1874–1881. IEEE, 2014.
- [7] S. Lee, G. Bekey, and A. Bejczy. Computer control of space-borne teleoperators with sensory feedback. In *Proceedings. 1985 IEEE International Conference on Robotics and Automation*, volume 2, pages 205–214, Mar 1985.
- [8] Philip S Green, John W Hill, Joel F Jensen, and A Shah. Telepresence surgery. *IEEE Engineering in Medicine and Biology Magazine*, 14(3):324–329, 1995.
- [9] Carsten Preusche, Tobias Ortmaier, and Gerd Hirzinger. Teleoperation concepts in minimal invasive surgery. *Control engineering practice*, 10(11):1245–1250, 2002.
- [10] N.G.Tsagarakis, D.G.Caldwell, A. Bicchi, F. Negrello, W. Choi M. Garabini, L. Baccelliere, V.G. Loc, J. Noorden, M. Catalano, M. Ferrati, L. Muratore, A. Margan, L. Natale, E. Mingo, H. Dallali, A. Settimi, A. Rocchi, V. Varricchio, L. Pallottino, C. Pavan, A. Ajoudani, Jinh Lee, P. Kryczka, and D. Kanoulas. Walk-man: A high performance humanoid platform for realistic environments. *Journal of Fields Robotics*, 2017 (IN PRESS).
- [11] C. Baggio, A. Bernardini, R. Colozza, L. Corazza, M. Della Bella, G. Di Pasquale, M. Dolce, A. Goretti, A. Martinelli, G. Orsini, et al. Field manual for post-earthquake damage and safety assessment and short term countermeasures (aedes). 2007.
- [12] M. G. Catalano, G. Grioli, E. Farnioli, A. Serio, C. Piazza, and A. Bicchi. Adaptive Synergies for the Design and Control of the Pisa/IIT SoftHand. *International Journal of Robotics Research*, 33:768–782, 2014.
- [13] A. Settimi, C. Pavan, V. Varricchio, M. Ferrati, E. Mingo Hoffman, A. Rocchi, K. Melo, N. G Tsagarakis, and A. Bicchi. A Modular Approach for Remote Operation of Humanoid Robots in Search and Rescue Scenarios. In *International Workshop on Modelling and Simulation for Autonomous Systems*, pages 192–205. Springer International Publishing, 2014.
- [14] Sebastian OH Madgwick. An efficient orientation filter for inertial and inertial/magnetic sensor arrays. *Report x-io and University of Bristol (UK)*, 2010.
- [15] Changmok Choi and Jung Kim. Synergy matrices to estimate fluid wrist movements by surface electromyography. *Medical engineering & physics*, 33(8):916–923, 2011.
- [16] A. Ajoudani, S. B. Godfrey, M. Catalano, G. Grioli, N. G. Tsagarakis, and A. Bicchi. Teleimpedance control of a synergy-driven anthropomorphic hand. In *2013 IEEE/RSJ International Conference on Intelligent Robots and Systems*, pages 1985–1991, Nov 2013.
- [17] Andy Cheung. The effect of visuohaptic delays on task performance and human control strategy in manual control tasks. 2016.
- [18] Luca Muratore, Arturo Laurenzi, Enrico Mingo Hoffman, Alessio Rocchi, Darwin G Caldwell, and Nikos G Tsagarakis. XBotCore: A Real-Time Cross-Robot software platform. In *ICRC17, 2017 IEEE International Conference on Robotic Computing*, 2017.
- [19] Giorgio Metta, Paul Fitzpatrick, and Lorenzo Natale. Yarp: Yet another robot platform. *International Journal on Advanced Robotics Systems*, 2006.
- [20] Martin A Fischler and Robert C Bolles. Random sample consensus: a paradigm for model fitting with applications to image analysis and automated cartography. *Communications of the ACM*, 24(6):381–395, 1981.
- [21] Sebastian OH Madgwick, Andrew JL Harrison, and Ravi Vaidyanathan. Estimation of IMU and MARG Orientation using a Gradient Descent Algorithm. In *IEEE International Conference on Rehabilitation Robotics*, pages 1–7, 2011.

- [22] S. Kohlbrecher, J. Meyer, O. von Stryk, and U. Klingauf. A flexible and scalable slam system with full 3d motion estimation. In *Proc. IEEE International Symposium on Safety, Security and Rescue Robotics (SSRR)*. IEEE, November 2011.
- [23] Radu Bogdan Rusu and Steve Cousins. 3D is here: Point Cloud Library (PCL). In *Proceedings of the IEEE International Conference on Robotics and Automation (ICRA)*, Shanghai, China, 2011.
- [24] Dimitrios Kanoulas and Marsette Vona. The Surface Patch Library (SPL). In *In the 2014 IEEE ICRA Workshop: MATLAB/Simulink for Robotics Education and Research*, 2014. <http://ccis.neu.edu/research/gpc/spl>.